Hydrogen bonding in phthalimido carboxylic acids: cyclic voltammetric study and correlation with photochemical reactivity. Part 2.[1] Aliphatic and aromatic acids †

Michael Oelgemöller,*[a] Andreas Haeuseler,*[b] Michael Schmittel,*[b] Axel G. Griesbeck,[c] Johann Lex[c] and Yoshihisa Inoue[a]

[a] *Inoue Photochirogenesis Project, ERATO, JST, 4-6-3 Kamishinden, Toyonaka-shi, Osaka, 560-0085, Japan*
[b] *FB 8 - OC1 (Chemie-Biologie) der Universität-GH Siegen, Adolf-Reichwein-Straße 2, D-57068 Siegen, Germany*
[c] *Institut für Organische Chemie, Universität zu Köln, Greinstraße 4, D-50939 Köln, Germany*

Received (in Cambridge, UK) 3rd July 2001, Accepted 9th January 2002

Cyclic voltammetry was applied as a useful tool for the detection and semiquantitative assessment of hydrogen bonding in phthalimidoalkyl and aryl carboxylic acids in solution. Both *intra-* and *intermolecular* hydrogen bonding could be detected and were assigned on the basis of base (DBU), acid (trifluoromethanesulfonic acid), solvent (MeCN *vs.* DMF), concentration and scan rate effects, as well as multisweep experiments. The observation of *intramolecular* hydrogen bonding neatly correlates with the reactivity pattern of the corresponding phthalimido carboxylic acids in photodecarboxylation reactions.

Introduction

Due to its unique importance in biology and chemistry[2] hydrogen bonding has been intensively studied by a broad variety of techniques. Among the well-established methods are, for example, IR spectroscopy,[3] calorimetry,[4] and NMR spectroscopy.[5] Recently, cyclic voltammetry (CV) was established as a powerful technique for the observation of *intermolecular* hydrogen bonding in solution.[6] During our ongoing study on the photochemical decarboxylation (PDC) of phthalimido alkyl carboxylates,[7,8] we have applied this technique for the analysis of *intramolecular* hydrogen bonds activating the imide electrophore/chromophore. Generally speaking, photochemical reactions can be influenced by hydrogen bonding,[9] which leads to either activation or deactivation of the photochemical step. The *one-way* photoisomerization of 2′-hydroxychalcone[10] can be seen as a representative example of the latter case, whereas hydrogen bond activation is assumed in case of the effective α-decarboxylation of phthaloyl amino acids.[11] Although the photochemistry[12] and electrochemistry[13] of phthalimides have been intensively investigated over the last decades, a direct correlation of photo- and electrochemical properties has not been reported so far.

Results and discussion

Three groups of phthalimido carboxylic acids were selected for CV measurements (Chart 1) differing in distance and flexibility of the linker separating the electrophore and carboxylic group: *aliphatic* (**1**–**7**), *aromatic* (**8**–**11**) and *heteroatom* substituted phthalimido carboxylic acids (**12** and **13**). The electrochemical properties of the sulfur-containing compounds **12** and **13** have recently been described,[14] and we will now present a detailed comparative study. For comparison, the methyl ester **14** and *N*-methylphthalimide **15** were additionally chosen.

The starting materials **1**–**11** were synthesized from phthalic anhydride and the corresponding amino acids by literature procedures.[15] The sulfur-containing derivatives **12** and **13** were prepared by a method described by Gong and Iwasawa,[16] compound **14** by methylation of the corresponding free acid **1**.[17] CV measurements were performed in acetonitrile for compounds **1**–**15** and additionally in DMF for **1**–**4**, **8**, **9**, **12** and **13**. In addition to the partial reversible reduction waves (corresponding to electron transfer to the radical anions) characterized by $E_{1/2}$, additional anodically shifted *pre*-waves E_{pc} (peak cathodic) were detected which can be related to hydrogen-bonded species. Due to the entailing partial protonation of the carbonyl group its acceptor strength is increased, and as result, an anodic shift of the corresponding wave was observed. Additional hydrogen bonding at the second carbonyl group of the phthalimide leads to an even more pronounced anodic shift.[18]

The observed *pre*-waves can be correlated with three limiting aggregation modes (Chart 2; shown prior to reduction): (**A**) *intermolecular*, (**B**) *intramolecular* and (**C**) a combination of *intra-* and *intermolecular* bonding, the latter accompanying **B** in non-polar and polar aprotic solvents. ‡ The well-known dimerization of carboxylic groups[19] is still assumed to be an important *intermolecular* interaction but since the electrophore is not involved in this *terminal* hydrogen-bonded aggregation these dimers will behave electrochemically similarly to **D**.

Evidence for the involvement of the depicted structures resulted from (*a*) the addition of base (DBU) and acid (trifluoromethanesulfonic acid, TFMSA), respectively. The *pre*-waves assigned to *intermolecular* hydrogen bonding (as in **A** and partly in **C**) decreased when DBU was added, whereas the addition of acid resulted in an increase in current height of wave **C** and a decrease of waves **B** and **D** due to the additional protonation of the *free* carbonyl functions.

(*b*) A similar dependence was found upon changing the solvent from acetonitrile to DMF. According to the hydrogen

---

† Electronic supplementary information (ESI) available: X-ray crystallographic data and cyclic voltammograms. See http://www.rsc.org/suppdata/p2/b1/b105860f/

‡ Additional types of aggregation with the electrophore (*e.g.* trimerization similar to **C**) might be involved but we assume that these aggregates are only populated in minor amounts.

DOI: 10.1039/b105860f

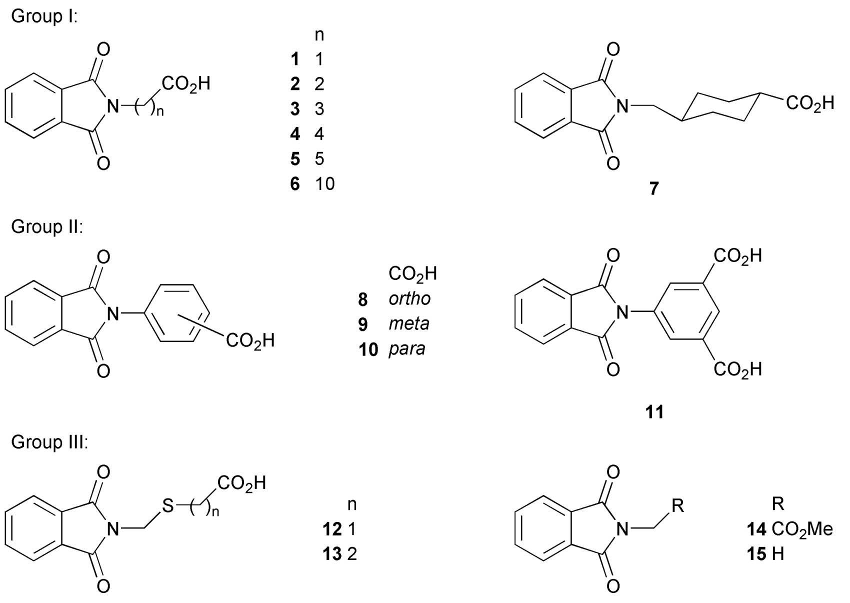

Chart 1

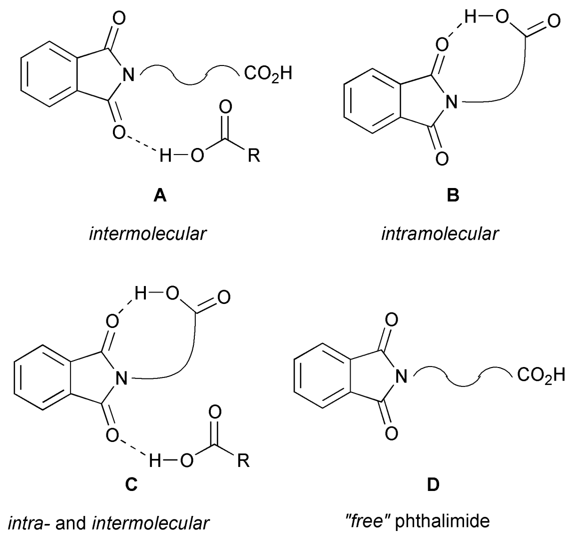

Chart 2

bond basicity scale,[20] DMF has about twice the hydrogen bond acceptor capabilities of MeCN. Hence, weaker *intermolecular* and *intramolecular* hydrogen bonds were suppressed in DMF due to stronger interactions with the solvent.

(*c*) A further assignment of the *inter-* and *intramolecular* nature of the *pre*-waves was obtained by variation of the substrate concentration and the scan rate during the CV measurements. Only the *intermolecular pre*-waves were influenced by these two parameters. Theoretical investigations by Savéant and Vianello have shown that the potentials of electroactive substrates in dimerization reactions (following a $C_{\mathrm{rev}}E$ mechanism) depend strongly on the substrate concentrations and the scan rate during the CV measurement whereas the current heights are not influenced by the equilibrium of the dimerization.[21]

(*d*) Multisweep cyclic voltammograms, combined with digital simulations allow an insight into the reactions following the primary reduction of the phthalimido electrophore. With an increasing number of cycles, the reaction products are enriched in the diffusion layer of the electrode which influences the experimental curve.

A qualitative assessment of the strength of the *intramolecular* hydrogen bonding can be made by judging the difference with respect to the reversible $E_{½}$ wave ($\Delta E = E_{½} - E_{\mathrm{pc}}$). To account for the scan rate dependence of the irreversible peak potentials E_{pc} on the rate of follow-up reaction, *i.e.* protonation of the phthalimide radical anions, we have to assume similar protonation rates which is rather plausible because of the small structural variations at the phthalimide core.

Aliphatic phthalimido carboxylic acids (1–7), methyl ester 14 and *N*-methylphthalimide 15

The aliphatic carboxylic acid derivatives **1**–**6** differ solely in the length of the carbon chain linking the electrophore and the carboxylic acid, thus allowing the study of the distance dependence of the *intramolecular* hydrogen bonding. Substrate **7** incorporates a *trans* 1,4-disubstituted cyclohexane as a spacer and is less conformationally flexible than the pentamethylene analogue **5**. The results of the CV measurements are shown in Fig. 1 and summarized in Table 1.§

The phthalimido carboxylic acids **1**–**3** showed two *pre*-waves upon reduction in acetonitrile which can be assigned to hydrogen bonding of type **C** and **B**, respectively. The differences (ΔE) between these *pre*-waves and the reduction potentials $E_{½}$ already indicated that the strength of hydrogen bonding decreases with increasing distance and consequently, *intramolecular* interactions were no longer observed for **4**–**7**. Evidence for this assignment came from the addition of DBU since the first *pre*-waves of **1**–**3** (assigned to **C**) and of **4**–**7** (assigned to **A**) vanished upon addition of base, whereas only a slight cathodic shift of *pre*-wave **B** of **1**–**3** was observed. For the methyl ester **14** or *N*-methylphthalimide **15** the hydrogen bonding sites were blocked or vanished, respectively, and consequently, solely the reversible reduction waves of the free electrophores were found at $E_{½} = -1.84$ and -1.89 V (Fig. 1h, i).

A strong and tight *intramolecular* hydrogen bond between the phthalimide carbonyl group and the carboxylic proton was postulated for the glycine derivative **1**. Although this structural element was not found in its *solid state* structure (or in other phthaloyl α-amino acids),[22] it was proved for related naphthalenecarboximides of glycine *in solution* by fluorescence measurements.[11a] The addition of 0.5 equivalents of base during the CV spectroscopy in MeCN entailed a significant decrease of

---

§ The reduction potential of **1**–**6** is increasingly shifted towards more anodic potential. This trend is counter-intuitive and equally not in line with AM1 calculated adiabatic and vertical electron affinities. Hence, it should arise from a solvation effect: with increasing methylene chain length the negative charge of the radical anion becomes more and more localized, allowing a stronger differential solvation (DMF > MeCN).

Table 1 Reduction potentials for **1**–**7**, **14** and **15**[a]

Compound	$E_{pc}(1)/V_{Fc}$	$I_{pc}(1)/I_{½}$	$E_{pc}(2)/V_{Fc}$	$I_{pc}(2)/I_{½}$	$E_{½}/V_{Fc}$
1	−1.40 (br, **C**)	0.35	−1.82 (**B**)	0.60	−2.01 (**D**)
1[b]	−1.52 (**C**)	0.70			−2.10 (**D**)
2	−1.40 (br, **C**)	0.35	−1.86 (**B**)	[c]	−1.94 (**D**)
2[b]	−1.90 (**B**)	[c]			−1.96 (**D**)
3	−1.70 (br, **C**)	0.32	−1.86 (**B**)	[c]	−1.93 (**D**)
3[b]	−1.88 (**B**)	[c]			−1.93 (**D**)
4	−1.45 (br, **A**)	0.26			−1.90 (**D**)
4[b]					−1.91 (**D**)
5	−1.55 (br, **A**)	0.35			−1.90 (**D**)
6	−1.50 (br, **A**)	0.25			−1.89 (**D**)
7	−1.44 (br, **A**)	0.27			−1.83 (**D**)
14					−1.84 (**D**)
15					−1.89 (**D**)

[a] V *vs.* ferrocene/ferrocenium (Fc) couple in MeCN; *ca.* 4 mM; scan rate $v = 100$ mV s^{-1}; supporting electrolyte: *n*-tetrabutylammonium hexafluorophosphate; br, broad. [b] In DMF. [c] As shoulders, affected by the $E_{½}$ wave.

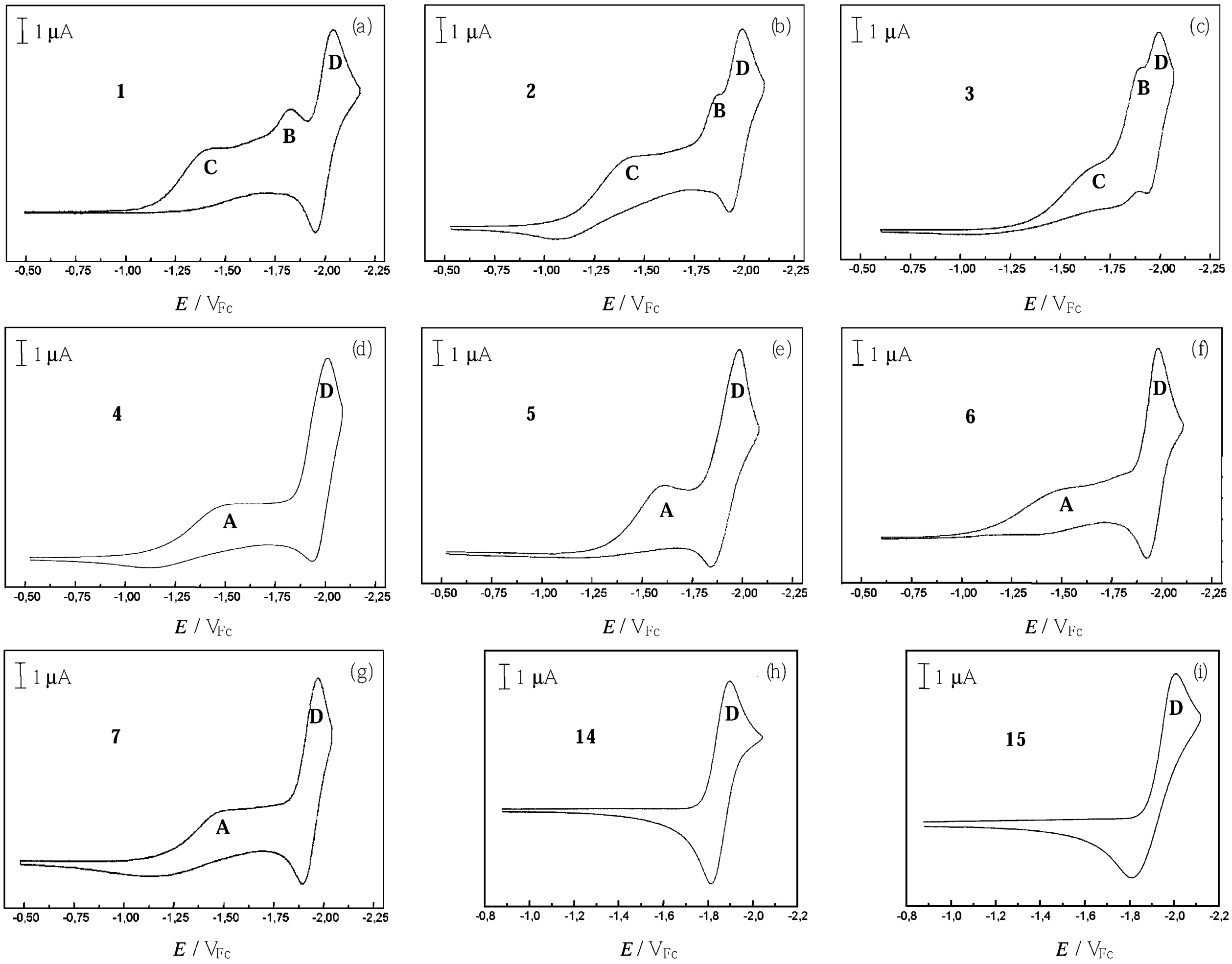

Fig. 1 Cyclic voltammograms for **1**–**7**, **14** and **15** in MeCN at $v = 100$ mV s^{-1}.

both, E_{pc}(**C**) and I_{pc}(**C**), leading to the disappearance of the wave after the addition of one equivalent (Fig. 2). Additionally, sharpening of wave **B** and a slight cathodic shift [ΔE_{pc}(**B**) = −0.04 V] were found upon addition of less than one equivalent of DBU. Even the addition of two equivalents of base did not decrease E_{pc}(**B**) significantly. Obviously, one of the carbonyl groups remains involved in a tight *intramolecular* interaction prior to reduction whereas all of the intermolecular hydrogen bonds have been disconnected.

While DBU is a strong base in water (pK_a = 12.9 of DBU·H$^+$)[23] with respect to an aliphatic carboxylic acid, it behaves differently in acetonitrile. In the latter solvent, the pK_a of free DBU·H$^+$ (23.9[24] respectively 24.1[25]) is so close to those of acetic acid (22.3[26]) and butyric acid (22.7[26]), respectively, that apparently the small driving force for deprotonation cannot overcome the stabilizing effect of the hydrogen bond. Thus, the DBU salt of **1** can be described as a hydrogen-bonded 1 : 1 complex between the substrate and DBU in which the carboxylic acid, its proton and the electrophore adopt a three-center hydrogen bond geometry (Scheme 1).[27]

In agreement with the model, the stepwise addition of TFMSA to **1** in acetonitrile led to an increase in the current height for E_{pc}(**C**) due to protonation by the acid (Fig. 3).

By lowering the concentration, however, *both* reduction waves showed a slight (*ca.* 20%) decrease in peak current ratio $I_{pc}/I_{½}$ along with broadening of the wave but with no clear

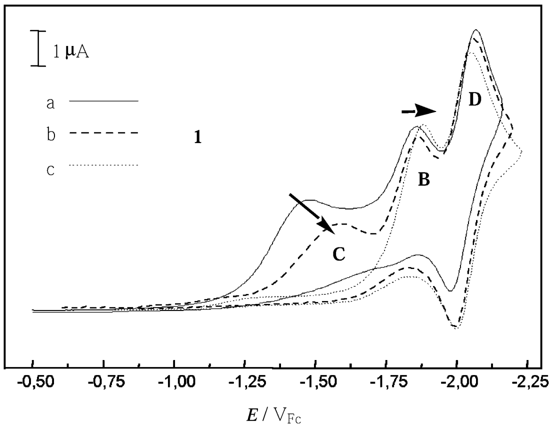

Fig. 2 CV of **1** in MeCN at v = 100 mV s^{-1} (a) prior to and after the addition of (b) 0.5 equiv. and (c) 1 equiv. of DBU.

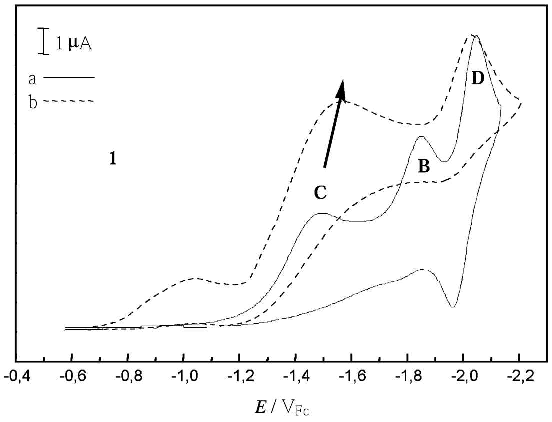

Fig. 3 CV of **1** in MeCN at v = 100 mV s^{-1} (a) prior and (b) after the addition of 0.5 equiv. of TFMSA.

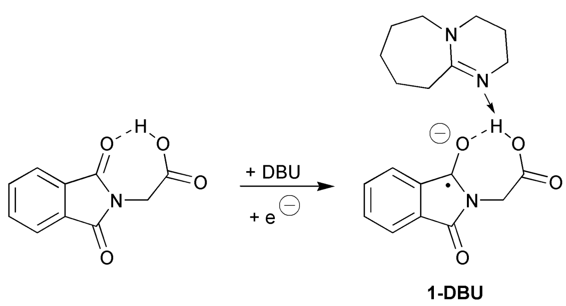

Scheme 1

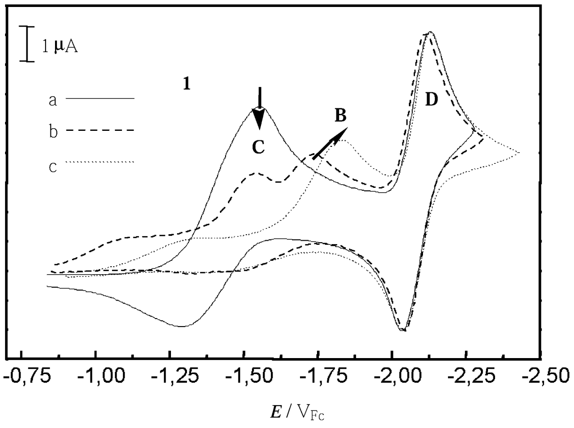

Fig. 4 CV of **1** at v = 100 mV s^{-1} (a) in DMF and after the addition of (b) 0.5 equiv. and (c) 1 equiv. of DBU.

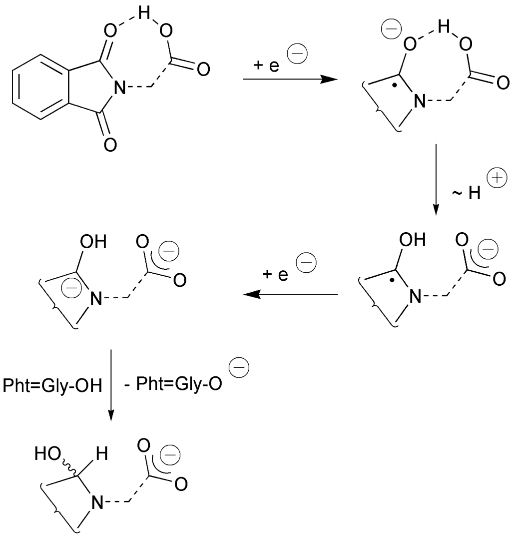

Scheme 2

cathodic shift.[21] This relative change is in line with an increased population of the *free* phthalimide structure **D**.

Further proof came from the analysis of the solvent dependency. In DMF, phthaloyl glycine **1** showed a single, strong *pre*-wave at $E_{pc} = -1.52$ V$_{Fc}$ (Fig. 4). In our previous report,[1] we have assigned this *pre*-wave to structure **B**, since in this strong hydrogen bond accepting solvent, intermolecular hydrogen bonds (as partly in structure **C**) might be suppressed due to interactions with the solvent molecules. Due to the large ΔE, the effect of base-addition and by comparison with compounds **2**, **3** and **8** (*vide infra*), we now assign it to the combined *intra*- and *intermolecular* hydrogen-bonded structure **C**. A dimerisation, including *intra*- and *intermolecular* hydrogen bonding, takes place due to a cooperative effect favoring structure **C** over **B**. Following this interpretation, no pure *intramolecular pre*-wave **B** was, however, observed in the cyclic voltammogram, but on stepwise addition of DBU, the intermolecular part in **C** became disrupted. Consequently, the intensity of the wave **C** dropped steadily, and a new *pre*-wave for pure **B** rose instead. After the addition of one equivalent of base only the *intramolecular pre*-wave remained at $E_{pc} = -1.83$ V$_{Fc}$ (Fig. 4c). Similar to the results obtained in acetonitrile, the formation of a DBU complex (Scheme 1) is likely due to the (most probably) comparable pK_a values of DBU and the carboxylic acid function.

Further evidence came from multisweep experiments as in both solvents the current heights dropped faster for the *pre*-waves than for the reversible $E_{½}$ (Fig. 5). This observation can be rationalized by a mechanism described by Leedy and Muck for the comparable reduction of *N*-methylphthalimide in the presence of phenol as a proton source.[13c] After reduction of the phthalimide to its radical anion, hydrogen bonds are involved in the protonation to the corresponding 3-hydroxyphthalimidine (Scheme 2; the dashed line between the electrophore and the carboxylic group represents *intra*- as well as *intermolecular* hydrogen bonds). As most of the negative charge of the delocalized radical anion resides at the carbonyl oxygen atoms (as shown in Scheme 2 for one carbonyl group),[28] the hydrogen bonds should become much stronger. Proton transfer will eventually follow to give the corresponding neutral hydroxyalkyl radical, which is more readily reduced than the phthalimide itself. The anion is finally protonated to afford 3-hydroxyphthalimidine. With an increasing number of cycles, the continuous consumption of protons near the electrode increases the pH and leads to the rapid disappearance of *pre*-waves **B** and **C**.

Compounds **2** and **3** also exhibited two *pre*-waves in acetonitrile which were assigned (in analogy to the glycine derivative **1**) as E_{pc}(**C**) and E_{pc}(**B**), respectively (Figs. 1b and c).

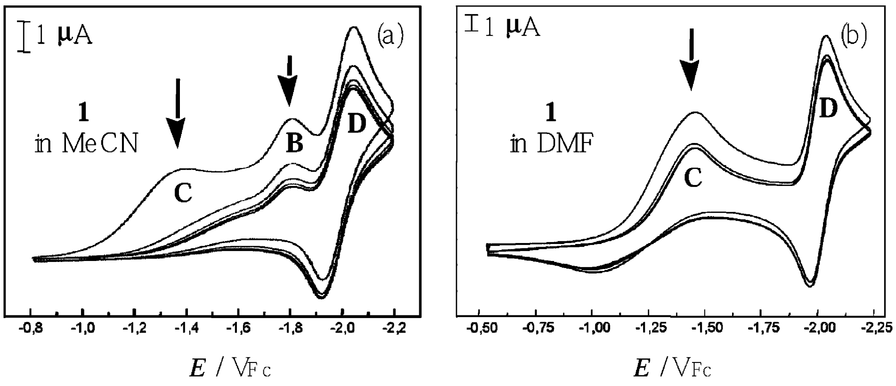

Fig. 5 Multisweep CV of **1** at $v = 100$ mV s^{-1} (a) in MeCN and (b) in DMF.

For *N*-phthaloyl-β-alanine **2**, addition of one equivalent of DBU resulted in complete disappearance of E_{pc}(**C**), whereas the second, much sharper E_{pc}(**B**) remained but was slightly shifted. In the case of the γ-aminobutyric acid **3**, *both pre*-waves were affected by DBU and finally only the $E_{½}$ wave was recorded (Fig. 6). The different sensitivity towards base for **1**–**3** indicates that the strength of *intramolecular* hydrogen bonding decreases on going from the methylene (as for **1**) to the propylene (as for **3**) linker.

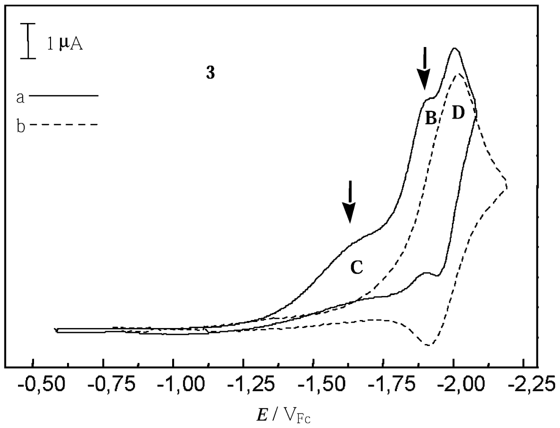

Fig. 6 CV of **3** in MeCN at $v = 100$ mV s^{-1} (a) prior to and (b) after the addition of 1 equiv. of DBU.

In DMF, only single *pre*-waves, in addition to the reversible reduction wave $E_{½}$, were detected for **2** and **3** but in comparison to **1** their ΔE values were drastically decreased. This result accounts for a change from the *inter*- and *intramolecular* hydrogen-bonded species **C** (for **1**) to a solely *intramolecular* bonded structure **B** for **2** and **3**, caused by a thermodynamically less favoured dimer formation for the benefit of intermolecular hydrogen bonding with DMF and further indicates the decrease of hydrogen bonding strength with increasing distance. Addition of DBU in DMF led to the total disappearance of the wave **B** for **2** and **3** without formation of new *pre*-waves in line with the behavior of the *intermolecular* bonds in acetonitrile. In the course of the multisweep experiments for **2** and **3** in DMF, the *pre*-waves decreased faster than the reversible $E_{½}$ waves showing that proton transfer through *intramolecular* hydrogen bonds is involved in further reduction steps (Scheme 2).

With further elongated linker chains (Figs. 1d–g) only single *intermolecular pre*-waves assigned to type **A** could be observed for **4**–**7**, which disappeared totally upon addition of one equivalent of DBU in all cases. For compounds **4** and **5**, the E_{pc}(**A**) *pre*-waves are more pronounced than for **6** indicating that the increased flexibility due to the longer carbon chain prevents aggregation.[29] After the addition of one equivalent of TFMSA to **6** in MeCN only E_{pc}(**A**) was detectable. When the concentration (Fig. 7) and scan rate dependence was measured for substrate **7**, the amount of I_{pc} in comparison to $I_{½}$ decreased upon dilution or at higher scan rates presenting another hint for the intermolecular aggregation of **7**.[21]

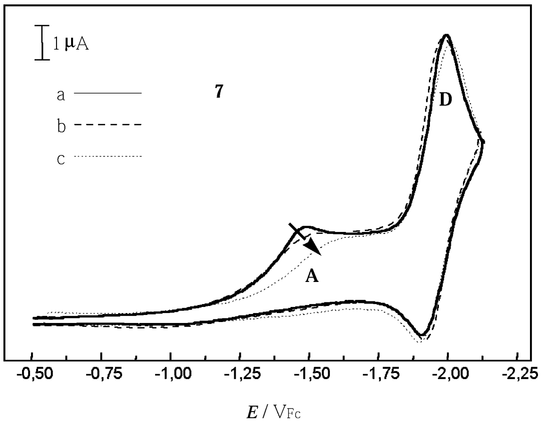

Fig. 7 Concentration dependence for **7** in MeCN at $v = 100$ mV s^{-1}, (*a*) 8.4 μM, (*b*) 4.2 μM and (*c*) 2.8 μM.

The distance dependence of hydrogen bonding also became obvious from the differences between E_{pc} and the reversible $E_{½}$ wave. For **1**–**3**, $\Delta E = E_{½} - E_{pc}(\mathbf{B})$ dropped slightly in both solvents on changing from the methylene to the ethylene or propylene linker. For **4**–**7** in MeCN, $\Delta E = E_{½} - E_{pc}(\mathbf{A})$ remained almost constant showing that the intermolecular interaction is influenced less by structural differences. Especially interesting in this context is a comparison with the photochemical behavior of the phthalimido carboxylic acids **1**–**7**. Compound **1** undergoes clean and efficient α-photodecarboxylation (PDC) when irradiated in several organic solvents.[11,30] This correlates nicely with a tight *intramolecular* hydrogen bond observed in the cyclic voltammograms recorded both in acetonitrile and DMF, and accounts for an *excited state proton transfer* (ESPT)[31] mechanism (Scheme 3). Further evidence came from related naphthalene carboximides of glycine, as these compounds showed an enhancement of their fluorescence efficiencies[11a] indicating hydrogen bonding between the side chain carboxy and imide carbonyl groups[32] (**1** itself shows only very weak fluorescence[33]). The photochemical reactivity of the β-alanine derivative **2** reported in literature is, however, contradictory. Yoon *et al.* recently described the formation of decarboxylation products in moderate yields during the photolysis of **2** in acetonitrile[34] whereas no reactivity was described for irradiation in acetone.[8d] This different behavior can be explained by a higher solvent sensitivity of the *intramolecular* hydrogen bonding for compound **2**. Indeed, in comparison with **1**, the corresponding *pre*-wave of **2** is less pronounced in acetonitrile and further weakened in hydrogen bonding accepting solvents like DMF (CV) or acetone (photolysis). Thus, β-decarboxylation is (at least) partly observable in MeCN but *not* in acetone.

Table 2 Reduction potentials for **8**–**11**[a]

Compound	$E_{pc}(1)/V_{Fc}$	$I_{pc}(1)/I_{½}$	$E_{pc}(2)/V_{Fc}$	$I_{pc}(2)/I_{½}$	$E_{½}/V_{Fc}$
8	−1.40 (br, **C**)	0.35	−1.81 (**B**)	0.60	−2.02 (**D**)
8[b]	−1.77 (br, **C**)	0.50	−1.95 (**B**)	0.45	−2.16 (**D**)
9		−1.40 to −1.50 (br, **A**)[c]		0.30	−1.88 (**D**)
9[b]	−1.80 (**B**)	[d]			−1.96 (**D**)
10	−1.50 (br, **A**)	0.30			−1.84 (**D**)
11[e]		−1.55 (br, **A**)[c]		0.80	−1.86 (**D**)

[a] V *vs.* ferrocene/ferrocenium (Fc) couple in MeCN; *ca.* 4 mM; scan rate $v = 100$ mV s^{-1}; supporting electrolyte: *n*-tetrabutylammonium hexafluorophosphate; br, broad. [b] In DMF. [c] Overlapping of several *pre*-waves. [d] As shoulders, affected by the $E_{½}$ wave. [e] Low solubility.

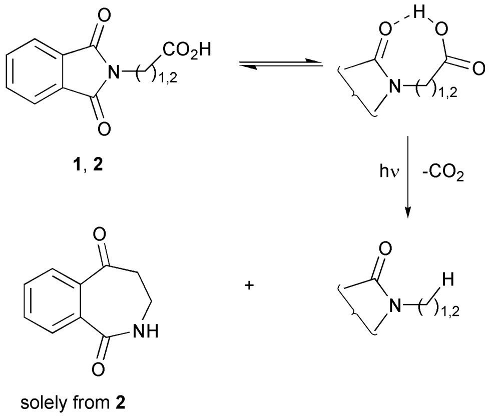

Scheme 3

The butyric acid derivative **3** is photostable upon photolysis in acetone[11] but undergoes C–H activation reactions in acetonitrile.[34] Obviously, further elongation of the carbon linker decreases the efficiency for photochemical decarboxylation reactions and favors alternative reaction channels or deactivation processes. An explanation is the weak or missing hydrogen bond for efficient ESPT. Consequently, the phthalimides **4**–**6** are photochemically inert but can be activated for PDC by transformation into the corresponding potassium carboxylates.[8] As an explanation for the high efficiency and selectivity of this activating process a potassium cation mediated preorientation was postulated in the ground and excited states independent of the distance.[35]

Phthalimidoarenecarboxylic acids (8–11)

In the aromatic carboxylic acid derivatives **8**–**10** the carboxylic acid group is attached at different positions relative to the electrophore. Due to the low flexibility and the preferred twisted orientation of phthalimide and the phenyl ring[36] this arrangement is expected to cause different CV behavior if compared with the conformationally more flexible compounds **2**–**4**, **12** and **13** (*vide infra*). Additionally, the stiff geometry should allow the formation of smaller aggregates. Substrate **11** carries a second carboxylic acid group in the *meta*-position and was expected to show an even more pronounced hydrogen bond activity. The results of the CV measurements are shown in Fig. 8 and summarized in Table 2.

At low scan rates (>20 mV s^{-1}) in acetonitrile, compounds **8**–**11** showed reversible reduction waves and additional anodically shifted *pre*-waves due to hydrogen bonding.

In the case of phthaloylanthranilic acid **8** two *pre*-waves were detected indicating a strong tendency for the formation of *intramolecular* hydrogen bonds (Fig. 8a). In the multisweep experiment the ratio of current height $I_{pc}/I_{½}$ (for both **C** and **B**) decreased significantly after a few cycles due to the consumption of protons in further reactions of the generated radical anion (similar to Scheme 2). The addition of DBU led to a reduction of I_{pc}(**C**) which disappeared completely after one equivalent (Fig. 9). In contrast, the E_{pc}(**B**) wave was not affected in intensity but shifted slightly ($\Delta E = -0.11$ V), in line with a strong *intramolecular* interaction in **8** (as shown for **1** in Scheme 1).¶

The concentration dependence confirmed this hypothesis. Upon dilution, the first wave E_{pc}(**C**) showed a cathodic shift and decreased whereas the potential of the second wave E_{pc}(**B**) remained unchanged (Fig. 10).

Compared to its aliphatic analogue **2** the *intramolecular* hydrogen bond **B** appears to be much stronger in **8** which can be seen from ΔE of the corresponding *pre*-waves. Judging from the values of ΔE and $I_{pc}/I_{½}$ the strength of the hydrogen bonding of **8** is similar to that of the glycine derivative **1**. Obviously, the aromatic ring and the *ortho*-substitution lead to an optimal alignment of the electrophore and the carboxylic acid for tight hydrogen bonding. On basis of IR-spectroscopic measurements, *intramolecular* hydrogen bonding between the carbonyl group and carboxylic acid has also been reported for **8** and its transition metal complexes in the solid state.[37] In contrast to **1** (*vide supra*), two *pre*-waves were also observed in DMF (Fig. 12). Obviously, a change in the solvent does not affect the ability of **8** to form both hydrogen-bonded species **B** and **C**. A reasonable explanation might be the optimal geometry of phthaloylanthranilic acid for bifurcated (three-center) hydrogen bonds[38] and π-stacking,[39] which allows aggregation in solution. Support of this argumentation came from the X-ray structural analysis of **8** (Fig. 11),‖ as the molecules form hydrogen bonds between the carboxylic acid and the carbonyl groups (indicated by an arrow). The hydrogen atom is situated in one plane with the carboxylic function. This whole arrangement spans an angle of 28.8° with the isoindole plane of the next molecule.

Similar to the results obtained in acetonitrile, stepwise addition of base led to the total disappearance of the first *pre*-wave **C** whereas the *intramolecular* wave **B** shifted slightly towards $E_{pc}(\mathbf{B}) = -2.00\ V_{Fc}$. This (compared to **2**) different behavior in DMF could originate from the fixed geometry of electrophore and carboxylic group in **8** caused by the *ortho*-substituted arene. This arrangement allows only small changes in distance *via* rotation about the N–C bond. In terms of solvent mediated *intramolecular* electron transfer (ET) of U-shaped donor–acceptor systems, the term “bite size” was recently applied,[40] and adopting this model the “jaws” of the electrophore–carboxylic acid system open up in the order **8**, **1** and **2**.

The *meta*-linked substrate **9** showed a very broad *pre*-wave between $E_{pc} = -1.4$ and $-1.5\ V_{Fc}$ (Fig. 8b) assigned to structure **A**. Addition of one equivalent of base led to a significant decrease in height but even two equivalents did not cause its total disappearance. Since *intramolecular* hydrogen bonds are geometrically unlikely, this finding indicates that compound **9** can populate stable aggregates, *e.g. via* dimerization. Upon dilution, the *pre*-wave showed further broadening which

---

¶ Although benzoic acid (pK_a = 20.1) is a stronger acid in acetonitrile than acetic acid (22.3).[26]

‖ *Crystal data*: **8**, $C_{15}H_9NO_4$ (from acetone, mp 216–218 °C), M = 267.23, monoclinic, space group $P2_1/n$, a = 12.528(1), b = 7.897(1), c = 12.892(1) Å, β = 103.19(1)°; Mo-Kα radiation, 5224 reflections measured, $R_1 = 0.0369$, $wR_2 = 0.0920$ for 1982 reflections with $I > 2\sigma(I)$. CCDC reference number 166845. See http://www.rsc.org/suppdata/p2/b1/b105860f/ for crystallographic files in .cif or other electronic format.

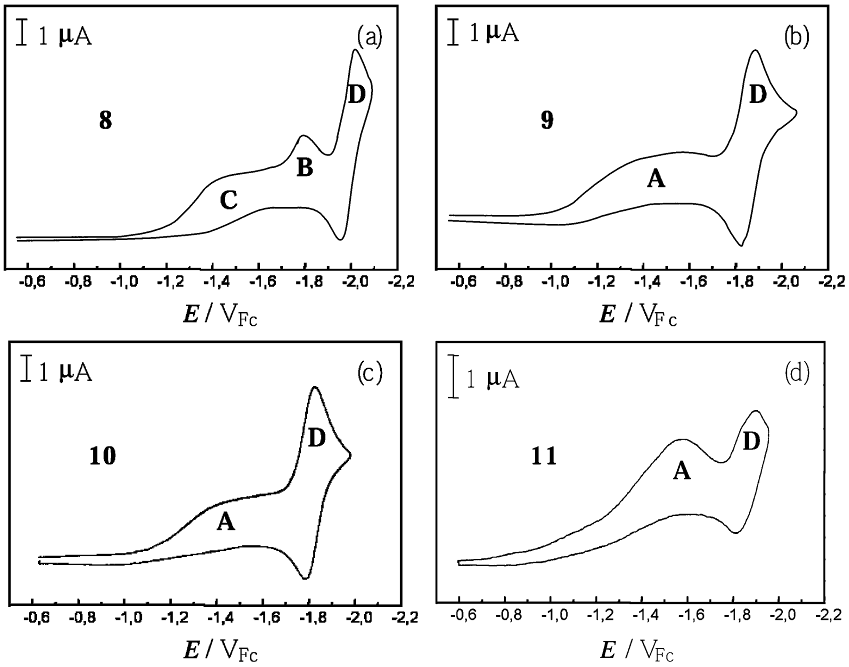

Fig. 8 Cyclic voltammograms for **8**–**11** in MeCN at $v = 100$ mV s^{-1}.

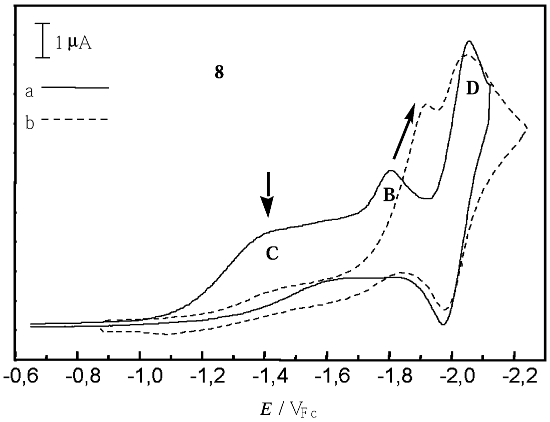

Fig. 9 CV of **8** in MeCN at $v = 100$ mV s^{-1} (a) prior to and (b) after the addition of 1 equiv. of DBU.

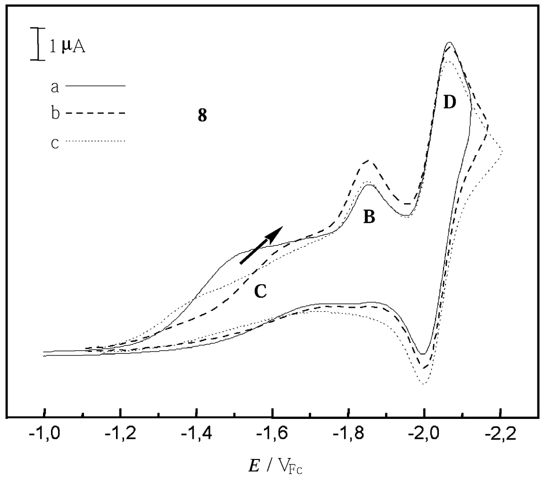

Fig. 10 Concentration dependence for **8** in MeCN at $v = 100$ mV s^{-1}, (a) 10.0 µM, (b) 5.3 µM and (c) 3.5 µM.

complicated the observation of a clear cathodic shift (similar to that found for **1**). In DMF, a weak *pre*-wave was found at $E_{pc} = -1.8$ V$_{Fc}$, which disappeared totally upon addition of DBU

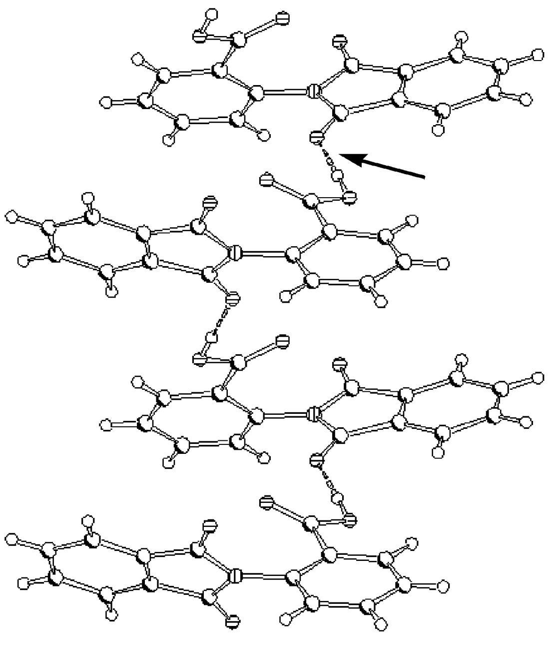

Fig. 11 Hydrogen bonding in **8** (X-ray).

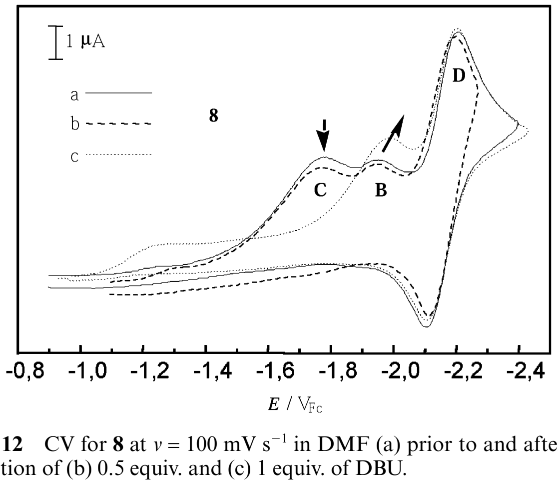

Fig. 12 CV for **8** at $v = 100$ mV s^{-1} in DMF (a) prior to and after the addition of (b) 0.5 equiv. and (c) 1 equiv. of DBU.

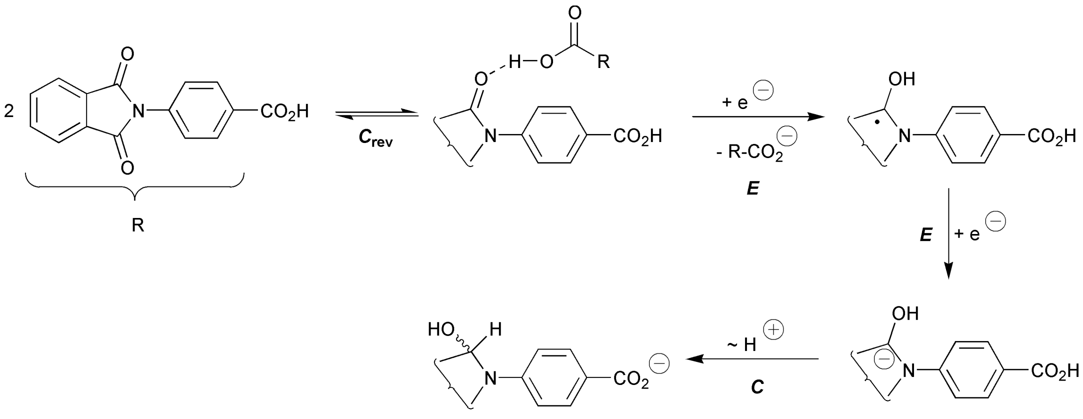

Scheme 4

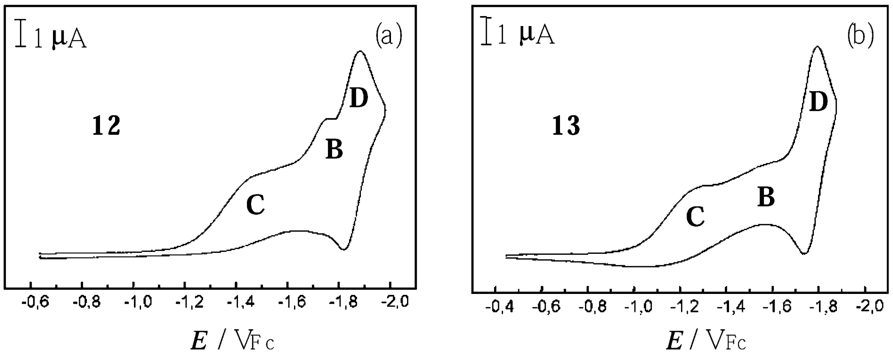

Fig. 13 Cyclic voltammograms for (a) **12** and (b) **13** in MeCN at $v = 100$ mV s^{-1}.

or in the multisweep experiment. As expected, interactions with the solvent DMF prevent the formation of stable aggregates of **9**.

The *para*-substituted derivative **10** gave only one broad *pre*-wave (Fig. 8c) which was totally suppressed by the addition of one equivalent of DBU. Based on its stiff geometry, this result indicates the E_{pc}(**A**) nature of the *pre*-wave. On lowering the concentration or increasing the scan rate a characteristic cathodic shift was detected.

Upon addition of TFMSA, the current height of the *pre*-wave increased and a second wave appeared at $E_{pc} = -0.8$ V_{Fc}. Due to the large anodic shift of *ca.* −1 V, it is assigned to a higher aggregated species with both carbonyl groups involved. In the multisweep experiment the *pre*-wave disappeared totally after a few cycles whereas its $E_{½}$ stayed almost constant. After the reduction of the phthalimide to the corresponding radical anion the *intermolecular* hydrogen bond is involved in a further reduction reaction to the corresponding 3-hydroxyphthalimidine (as shown *via* a C_{rev}*EEC*-mechanism in Scheme 4).

Due to the consumption of protons during the reduction the pH in the diffusion layer at the electrode increases with each cycle. Consequently, after a few cycles a *pre*-wave for an *intermolecular* hydrogen bond was no longer observed. A digital simulation of the multisweep cyclic voltammogram based on this C_{rev}*EEC*-mechanism showed reasonable agreement with the experimental trace.

The dicarboxylic acid derivative **11** showed solely a very broad *pre*-wave centered at *ca.* −1.55 V_{Fc} (Fig. 8d). The enlarged height of this *pre*-wave may in fact indicate that the additional carboxylic group leads to an increased population of hydrogen-bonded structures, and indeed, compared to the monoacid **9** the ratio of peak current $I_{pc}/I_{½}$ was almost doubled. Although the low solubility of this compound in acetonitrile prevented further studies, a similar behavior to that of **9** is expected.

The photodecarboxylation of the *free* aromatic acids is energetically disfavored, and therefore, photochemical studies have been described solely for the potassium salts of **8** and **10**, respectively. Whereas **8** showed efficient decarboxylation when irradiated in aqueous acetone as its potassium carboxylate,[41] the potassium salt of **10** remained photostable.[42] This different reactivity correlates convincingly with the results from the cyclic voltammetry study, as only compound **8** showed strong *intramolecular* hydrogen bonding as its *free* acid and DBU complex.

Phthalimidoalkylsulfanyl carboxylic acids (12, 13)

The sulfur-containing phthalimido carboxylic acids **12** and **13** differ only in the number of methylene groups separating the terminal carboxylic group and the heteroatom. We have shown that this different arrangement of the sulfur atom strongly influences the photochemical behavior of both compounds.[14] The electrochemical properties of substrates **12** and **13** were therefore investigated and the results of the CV measurements are summarized in Fig. 13 and Table 3.

Both mercaptocarboxylic acids showed partially reversible reduction waves even at low scan rates (>50 mV s^{-1}). Additionally, in acetonitrile two broad anodically shifted *pre*-waves could be detected, which account for *intra*- (**B**) and *intermolecular* (**C**) hydrogen bonding between the phthalimide and the carboxylic proton (Fig. 13a and b). The behavior is different on changing to DMF. Only **12** shows a single *pre*-wave, whereas for **13** none is detected. Independent of the solvent for both compounds the *pre*-waves disappeared completely when one equivalent of DBU was added.

Furthermore, the addition of TFMSA resulted in an increase of the current height of the first *pre*-wave **C**, and after the addition of more than two equivalents of acid only the E_{pc}(**C**) wave could be detected in both cases. Final proof for the assignment of the *inter*- and *intramolecular* nature of the *pre*-

Table 3 Reduction and oxidation potentials for **12** and **13**[a]

Compound	$E_{pc}(1)$ [V_{Fc}]	$I_{pc}(1)/I_{1/2}$	$E_{pc}(2)$ [V_{Fc}]	$I_{pc}(2)/I_{1/2}$	$E_{½}$ [V_{Fc}]	E_{pa} [V_{Fc}]
12	−1.50 (br, **C**)	0.36	−1.74 (**B**)	[b]	−1.87 (**D**)	+1.94
12[c]			−1.77 (**B**)	[b]	−1.87 (**D**)	—[d]
13	−1.23 (br, **C**)	0.31	−1.50 (**B**)	[b]	−1.77 (**D**)	+1.86
13[c]					−1.83 (**D**)	—[d]

[a] V *vs.* ferrocene/ferrocenium (Fc) couple in MeCN; *ca.* 4 mM; scan rate $v = 100$ mV s^{-1}; supporting electrolyte: *n*-tetrabutylammonium hexafluorophosphate; br, broad. [b] As shoulders, affected by the $E_{½}$ wave. [c] In DMF. [d] Potential higher than the potential window of the solvent.

waves was obtained by varying the substrate concentration and the scan rate in the CV measurements. Only the first *pre*-wave E_{pc}(**C**) depended on these two parameters, as at lower concentrations and higher scan rates, a cathodic shift of E_{pc}(**C**) was observed, whereas the potential of E_{pc}(**B**) did not change.

This observation agrees with the observed photodecarboxylative activity of the mercaptoacetic acid **12**. Compared to the carboxylate (in MeCN: $E_{pa} \gg +2.0$ V_{Fc}) the thioether fragment is preferentially oxidized due to its lower lying oxidation potential (Table 3). Even at very high scan rates (up to 20000 V s^{-1}) only *irreversible* oxidation waves could be obtained for both compounds **12** and **13**, respectively. This finding accounts for fast follow-up reactions of the sulfur radical cation after the electron transfer step. For mercaptoacetic acid derivatives like **12** decarboxylation products were found in moderate to good yields besides the photoproducts arising from sulfur oxidation and α-proton rearrangement.[43] A reasonable explanation is the formation of an *intramolecular* hydrogen bond which assists proton transfer from the terminal carboxylic acid prior to effective *sulfur*-assisted α-decarboxylation (Scheme 5).[44] On the other hand, compound **13** showed much lower photoactivity even after transformation into its potassium salt.[14] The sulfur radical cation of the mercaptopropionic acid **13** cannot directly eliminate carbon dioxide and thus, is mainly deactivated by back electron transfer.

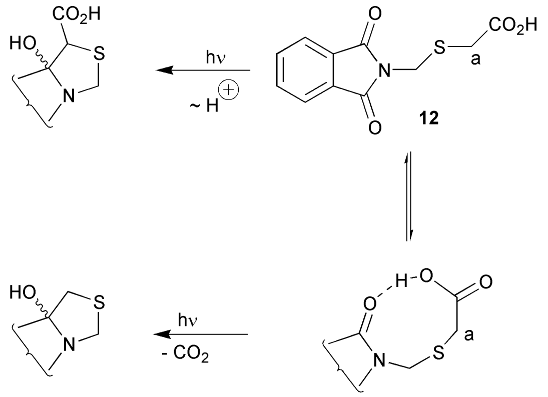

Scheme 5

Remarkably, ΔE for both *pre*-waves is larger for substrate **13** than for **12**, which may be explained by assuming that in the case of **13** the sulfur is involved in the hydrogen bonding with formation of two six-membered rings (Chart 3). Such a structure is more unlikely for the shorter derivative **12** and therefore, the missing influence of the sulfur atom leads to a less pronounced ΔE-shift.

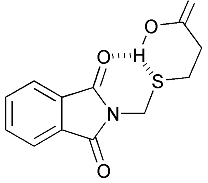

13

Chart 3

Conclusions

We investigated the electrochemical behavior of several aliphatic, as well as aromatic, phthalimido carboxylic acids by cyclic voltammetry. Focusing on the influence of hydrogen bonding between the phthalimido and the carboxylic moiety on the reduction potential of the electrophore, it was possible to estimate the strength and the origin of the hydrogen bonds. Depending on the interactions present, *pre*-waves emerged in the cyclic voltammogram shifted anodically with regard to the reduction wave of the free phthalimido carboxylic acid. *Pre*-waves caused by *inter*- and *intramolecular* hydrogen bonding could be identified by scan rate, concentration and solvent-dependent CV experiments, as well as by the addition of base or acid. The obtained results from these electrochemical measurements correlate with the photochemical behavior of the substrates, showing that hydrogen bonding strongly influences the reactivity pattern in the photodecarboxylation reaction of phthalimido carboxylic acids.

Experimental

Syntheses

Compounds **1**–**11** were synthesized by literature procedures from phthalic anhydride and the corresponding amino acids,[15] and have been described elsewhere.[8] The ester **14** was synthesized from **1** by methylation in MeOH and in the presence of catalytic amounts of sulfuric acid.[17] Compounds **12** and **13** were prepared from *N*-hydroxymethylphthalimide and the corresponding mercaptocarboxylic acid following the method of Gong and Iwasawa,[16] and have been described independently.[14] *N*-Methylphthalimide **15** was purchased from Aldrich.

Cyclic voltammetry[45]

Acetonitrile and DMF, both of HPLC grade, were distilled from CaH_2 under an inert atmosphere and filtered through basic alumina (ICN). The supporting electrolyte tetrabutylammonium hexafluorophosphate (purris. electrochemical grade, Fluka) was used without further purification. Benzoic acid and 1,8-diazabicyclo[5.4.0]undec-7-ene (DBU) were purchased from Aldrich, trifluoromethanesulfonic acid from Fluka.

A Princeton Applied Research Model 362 potentiostat with a Philips model PM 8271 XYt-recorder was used for scan rates <1 V s^{-1}. For fast scan cyclic voltammetry a Hewlett Packard Model 331A4 Function Generator was used connected to a three-electrode potentiostat developed by Amatore *et al.*[46] Data were recorded using an HP 54510 A digitizing oscilloscope linked to a 486DX33 computer using the HP data transfer program Scopelink. The ratios I_{pc}/I_{pa} were determined according to the equation of Nicholson.[47] All potentials were referenced to internal ferrocene.[48]

Digital simulation

Computer simulation of the redox chemistry of compound **10** was carried out using the Crank–Nicholson technique[49] and the program DigiSim.[50] The simulation of a full-cycle voltammogram consisted of 1000 data points, allowing an acceptable resolution of the cyclic voltammogram. All chemical reaction steps were assumed to be reversible except for the ET steps. The rate constants for the chemical reaction steps were varied using a standard heterogeneous electron transfer constant of $k^{\circ}_{\text{het.}}$ = 1 cm s^{-1} and a standard diffusion coefficient of $D = 10^{-5}$ cm^2 s^{-1}. This allows the achievement of the best possible agreement with the experimental curves.

Acknowledgements

This research project was financially supported by the Deutsche Forschungsgemeinschaft, the Fonds der Chemischen Industrie, the Volkswagenstiftung, Bayer AG and Merck KGaA. This paper is dedicated to Professor A. Maercker on the occasion of his 70th birthday.

References

1 Part 1. M. Oelgemöller, A. G. Griesbeck, J. Lex, A. Haeuseler, M. Schmittel, M. Niki, D. Hesek and Y. Inoue, *Org. Lett.*, 2001, **3**, 1593.

2 (*a*) G. A. Jeffrey and W. Saenger, *Hydrogen Bonding in Biological Structures*, Springer, Berlin, 1991; (*b*) G. A. Jeffrey, *An Introduction to Hydrogen Bonding*, Oxford University Press, New York, 1997; (*c*) S. Schreiner, *Hydrogen Bonding*, Oxford University Press, New York, 1997; (*d*) P. A. Kollman and L. C. Allen, *Chem. Rev.*, 1972, **72**, 283.

3 (*a*) P. Hobza and Z. Havlas, *Chem. Rev.*, 2000, **100**, 4253; (*b*) M. C. R. Symons, *Chem. Soc. Rev.*, 1983, **12**, 1; (*c*) A. N. Egorochkin and S. E. Skobeleva, *Russ. Chem. Rev.*, 1979, **48**, 1198; (*d*) M. Tichy, *Adv. Org. Chem.*, 1965, **5**, 115; (*e*) H. S. Aaron, *Top. Stereochem.*, 1979, **11**, 1.

4 (*a*) E. M. Arnett, L. Joris, E. Mitchell, T. S. S. R. Murty, T. M. Gorrie and P. v. R. Schleyer, *J. Am. Chem. Soc.*, 1970, **92**, 2365; (*b*) M. V. Rekharsky and Y. Inoue, *J. Am. Chem. Soc.*, 2000, **122**, 4418; (*c*) M. V. Rekharsky and Y. Inoue, *Chem. Rev.*, 1998, **98**, 1875.

5 (*a*) E. Chiarparin, S. Rüdisser and G. Bodenhausen, *ChemPhysChem*, 2001, 41; (*b*) A. Bagno, S. Gerard, J. Kevelam, E. Menna and G. Scorrano, *Chem. Eur. J.*, 2000, **6**, 2915; (*c*) W. D. Arnold and E. Oldfield, *J. Am. Chem. Soc.*, 2000, **122**, 12835; (*d*) J. C. Davis Jr. and K. K. Deb, *Adv. Magn. Reson.*, 1970, **4**, 201.

6 (*a*) Y. Ge, L. Miller, T. Ouimet and D. K. Smith, *J. Org. Chem.*, 2000, **65**, 8831; (*b*) Y. Ge and D. K. Smith, *Anal. Chem.*, 2000, **72**, 1860; (*c*) M. D. Greaves, A. Niemz and V. M. Rotello, *J. Am. Chem. Soc.*, 1999, **121**, 266; (*d*) A. Niemz and V. M. Rotello, *Acc. Chem. Res.*, 1999, **32**, 44; (*e*) R. Deans, A. Niemz, E. C. Breinlinger and V. M. Rotello, *J. Am. Chem. Soc.*, 1997, **119**, 10863; (*f*) N. Gupta and H. Linschitz, *J. Am. Chem. Soc.*, 1997, **119**, 6384; (*g*) Y. Ge, R. R. Lilienthal and D. K. Smith, *J. Am. Chem. Soc.*, 1996, **118**, 3976.

7 For *intermolecular* addition reactions, see: (*a*) A. G. Griesbeck, M. Oelgemöller and J. Lex, *Synlett*, 2000, 1455; (*b*) A. G. Griesbeck and M. Oelgemöller, *Synlett*, 2000, 71; (*c*) A. G. Griesbeck and M. Oelgemöller, *Synlett*, 1999, 492.

8 For *intramolecular* macrocyclisations, see: (*a*) A. G. Griesbeck, W. Kramer and M. Oelgemöller, *Synlett*, 1999, 1169; (*b*) W. Kramer, A. G. Griesbeck, F. Nerowski and M. Oelgemöller, *J. Inf. Rec.*, 1998, **24**, 81; (*c*) A. G. Griesbeck, A. Henz, W. Kramer, J. Lex, F. Nerowski, M. Oelgemöller, K. Peters and E.-M. Peters, *Helv. Chim. Acta*, 1997, **80**, 912; (*d*) A. G. Griesbeck, A. Henz, K. Peters, E.-M. Peters and H. G. von Schnering, *Angew. Chem.*, 1995, **107**, 498 (*Angew. Chem., Int. Ed. Engl.*, 1995, **34**, 474).

9 (*a*) J. L. Sessler, M. Sathiosatham, C. T. Brown, T. A. Rhodes and G. Wiederrecht, *J. Am. Chem. Soc.*, 2001, **123**, 3655; (*b*) A. Yokohama and K. Mizuno, *Org. Lett.*, 2000, **2**, 3457; (*c*) E. Prasad and K. R. Gopidas, *J. Am. Chem. Soc.*, 2000, **122**, 3191; (*d*) S. McN. Sieburth and K. F. McGee Jr., *Org. Lett.*, 1999, **1**, 1775; (*e*) D. A. Williamson and B. E. Bowler, *J. Am. Chem. Soc.*, 1998, **120**, 10902.

10 (*a*) Y. Norikane, H. Itoh and T. Arai, *Chem. Lett.*, 2000, 1094; (*b*) T. Arai and Y. Norikane, *Chem. Lett.*, 1997, 339.

11 (*a*) Y. Takahashi, T. Miyashi, U. C. Yoon, S. W. Oh, J. C. Sung, Y.-J. Lee, M. Mancheno, Z. Su, D. E. Falvey and P. S. Mariano, *J. Am. Chem. Soc.*, 1999, **121**, 3926; (*b*) A. G. Griesbeck and A. Henz, *Synlett*, 1994, 931; (*c*) Y. Sato, H. Nakai, T. Mizoguchi, M. Kawanishi, Y. Hatanaka and Y. Kanaoka, *Chem. Pharm. Bull.*, 1982, **30**, 1263.

12 (*a*) M. Oelgemöller, *EPA Newsl.*, 2000, **69**, 11; (*b*) A. G. Griesbeck, *Chimia*, 1998, **52**, 272; (*c*) J. D. Coyle, in *Synthetic Organic Photochemistry*, ed. W. M. Horspool, Plenum Press, New York, 1984, p. 259; (*d*) P. H. Mazzocchi, *Org. Photochem.*, 1981, **5**, 421; (*e*) Y. Kanaoka, *Acc. Chem. Res.*, 1978, **87**, 407.

13 (*a*) A. Orzeszko, J. K. Maurin, A. Niedzwiecka-Kornas and Z. Kazimierczuk, *Tetrahedron*, 1998, **54**, 7517; (*b*) J. D. Porter, S. Fletcher and R. G. Barradas, *J. Electrochem. Soc.*, 1979, **126**, 1693; (*c*) D. W. Leedy and D. L. Muck, *J. Am. Chem. Soc.*, 1971, **93**, 4264; (*d*) G. Farnia, A. Romanin, G. Capobianco and F. Torzo, *J. Electroanal. Chem.*, 1971, **33**, 31; (*e*) G. Capobianco, G. Farnia and F. Torzo, *Ric. Sci.*, 1968, **38**, 842.

14 A. G. Griesbeck, M. Oelgemöller, J. Lex, A. Haeuseler and M. Schmittel, *Eur. J. Org. Chem.*, 2001, 1831.

15 (*a*) A. G. Griesbeck, J. Hirt, K. Peters, E.-M. Peters and H. G. von Schnering, *Chem. Eur. J.*, 1996, **2**, 1388; (*b*) T. Vidal, A. Petit, A. Loupy and R. N. Gedye, *Tetrahedron*, 2000, **56**, 5473; (*c*) D. A. A. Kidd and F. E. King, *Nature (London)*, 1948, **162**, 776.

16 Y.-D. Gong and N. Iwasawa, *Chem. Lett.*, 1994, 2139.

17 G. B. Crippa and P. Galimberti, *Gazz. Chim. Ital.*, 1933, **63**, 81.

18 J. D. Carr, L. Lambert, D. E. Hibbs, M. B. Hursthouse, K. M. Abdul Malik and J. H. Tucker, *Chem. Commun.*, 1997, 1649.

19 (*a*) V. R. Thalladi, M. Nüsse and R. Boese, *J. Am. Chem. Soc.*, 2000, **122**, 9227; (*b*) L. Leiserowitz, *Acta Crystallogr., Sect. B*, 1976, **32**, 775; (*c*) D. Hadzi and S. Detoni, in *The Chemistry of Acid Derivatives*, ed. S. Patai, Wiley, New York, 1979, pt. 1, p. 213.

20 (*a*) M. H. Abraham and J. A. Platts, *J. Org. Chem.*, 2001, **66**, 3484; (*b*) M. H. Abraham, *Chem. Soc. Rev.*, 1993, **22**, 73; (*c*) M. J. Kamlet, J.-L. M. Abbound, M. H. Abraham and R. W. Taft, *J. Org. Chem.*, 1983, **48**, 2877.

21 J. M. Savéant and E. Vianello, *Electrochim. Acta*, 1967, **12**, 1545.

22 (*a*) N. Feeder and W. Jones, *Acta Crystallogr., Sect. C*, 1994, **50**, 820; (*b*) F. Kazmierczak, K. Gawronska, U. Rychlewska and J. Gawronski, *Tetrahedron: Asymmetry*, 1994, **5**, 527; (*c*) A. G. Michel and F. Durant, *Bull. Soc. Chim. Belg.*, 1975, **54**, 8403.

23 I. Hermecz, *Adv. Heterocycl. Chem.*, 1987, **42**, 83.

24 (*a*) A. Streitweiser and Y.-J. Kim, *J. Am. Chem. Soc.*, 2000, **122**, 11783; (*b*) W. Galezowski, A. Jarczewski, M. Stanczyk, B. Brzezinski, F. Bartl and G. Zundel, *J. Chem. Soc., Faraday Trans.*, 1997, **93**, 2515; (*c*) K. T. Leffek, P. Pruszynski and K. Thanapaalasingham, *Can. J. Chem.*, 1989, **67**, 590.

25 I. Kaljurand, T. Rodima, I. Leito, I. A. Koppel and R. Schwesinger, *J. Org. Chem.*, 2000, **65**, 6202.

26 K. Izutsu, *Acid–Base Dissociation Constants in Dipolar Aprotic Solvents*, Blackwell, Oxford, 1990.

27 (*a*) A. Kraft, *J. Chem. Soc., Perkin Trans. 1*, 1999, 705; (*b*) N. Ono, T. Yamada, T. Saito, K. Tanaka and A. Kaji, *Bull. Chem. Soc. Jpn.*, 1978, **51**, 2401.

28 (*a*) A. G. Griesbeck, M. S. Gudipati, J. Hirt, J. Lex, M. Oelgemöller, H. Schmickler and F. Schouren, *J. Org. Chem.*, 2000, **65**, 7151; (*b*) M. Freccera, E. Fasani and A. Albini, *J. Org. Chem.*, 1993, **58**, 1740; (*c*) Y. Kubo, M. Nanba, E. Hayashi and T. Araki, *Bull. Chem. Soc. Jpn.*, 1989, **62**, 3972.

29 F. Eblinger and H.-J. Schneider, *Angew. Chem.*, 1998, **110**, 821 (*Angew. Chem., Int. Ed.*, 1998, **37**, 826).

30 U. C. Yoon, D. U. Kim, C. W. Lee, Y. S. Choi, Y.-J. Lee, H. L. Ammon and P. S. Mariano, *J. Am. Chem. Soc.*, 1995, **117**, 2698.

31 S. J. Formosinho and L. G. Arnaut, *J. Photochem. Photobiol., A*, 1993, **75**, 21.

32 (*a*) N. J. Turro, *Modern Molecular Photochemistry*, University Science Books, Mill-Valley, 1991; (*b*) R. A. Caldwell and R. P. Gajewski, *J. Am. Chem. Soc.*, 1971, **93**, 532.

33 (*a*) H. Görner, A. G. Griesbeck, T. Heinrich, W. Kramer and M. Oelgemöller, *Chem. Eur. J.*, 2001, **7**, 1530; (*b*) A. G. Griesbeck and H. Görner, *J. Photochem. Photobiol., A*, 1999, **129**, 111.

34 U. C. Yoon, C. W. Lee, S. W. Oh and P. S. Mariano, *Tetrahedron*, 1999, **55**, 11997.

35 (*a*) H. Jiang, H. Xu and J. Ye, *J. Chem. Soc., Perkin Trans. 2*, 2000, 925; (*b*) P. J. Wagner, *Acc. Chem. Res.*, 1983, **16**, 461.

36 (*a*) W. Kramer, PhD Thesis, University of Cologne, 2000; (*b*) S. Voliotis, J. M. Arrieta and G. Germain, *Acta Crystallogr., Sect. C*, 1984, **40**, 1946; (*c*) G. Bocelli and A. Cantoni, *Acta Crystallogr., Sect. C*, 1989, **45**, 1658; (*d*) G. Bocelli, A. Cantoni and P. Cozzini, *Acta Crystallogr., Sect. C*, 1995, **51**, 2372.

37 M. G. Abd El Wahed, K. El Manakhly, H. Hammad and A. Barakat, *Bull. Korean Chem. Soc.*, 1996, **17**, 285.

38 H. C. Strauch, T. Rinderknecht, G. Erker, R. Fröhlich, E. Wegelius, F. Zippel, S. Höppener, H. Fuchs and L. Chi, *Eur. J. Org. Chem.*, 2000, 187.

39 (*a*) E. Kim, S. Paliwal and C. S. Wilcox, *J. Am. Chem. Soc.*, 1998, **120**, 11192; (*b*) S. Paliwal, S. Gaib and C. S. Wilcox, *J. Am. Chem. Soc.*, 1994, **116**, 4497.

40 N. R. Lokan, M. N. Paddon-Row, M. Koeberg and J. W. Verhoeven, *J. Am. Chem. Soc.*, 2000, **122**, 5075.

41 A. G. Griesbeck, W. Kramer and J. Lex, *Angew. Chem.*, 2001, **113**, 586 (*Angew. Chem., Int. Ed.*, 2001, **40**, 577).

42 A. Henz, PhD Thesis, University of Würzburg, 1996.

43 A. G. Griesbeck, J. Hirt, W. Kramer and P. Dallakian, *Tetrahedron*, 1998, **54**, 3169.

44 (*a*) D. R. G. Brimage, R. S. Davidson and P. R. Steiner, *J. Chem. Soc., Perkin Trans. 1*, 1973, 526; (*b*) R. S. Davidson and P. R. Steiner, *J. Chem. Soc., Perkin Trans. 2*, 1972, 1357; (*c*) R. S. Davidson and P. R. Steiner, *J. Chem. Soc. C*, 1971, 1682.

45 M. Schmittel, A. Burghart, H. Werner, M. Laubender and R. Söllner, *J. Org. Chem.*, 1999, **64**, 3077.

46 C. Amatore, C. Lefrou and F. Pflügler, *J. Electroanal. Chem. Interfacial Electrochem.*, 1989, **270**, 43.

47 R. S. Nicholson, *Anal. Chem.*, 1966, 1406.

48 To obtain values *vs.* SCE, simply add +0.39 V.

49 (*a*) A. Lasia, *J. Electroanal. Chem. Interfacial Electrochem.*, 1983, **146**, 397; (*b*) J. Heinze, M. Störzbach and J. Mortensen, *J. Electroanal. Chem. Interfacial Electrochem.*, 1984, **165**, 61; (*c*) J. Heinze and M. Störzbach, *J. Electroanal. Chem. Interfacial Electrochem.*, 1993, **346**, 1.

50 (*a*) M. Rudolph, D. P. Reddy and S. W. Feldberg, *Anal. Chem.*, 1994, **66**, 589A; (*b*) M. Rudolph, *J. Electroanal. Chem. Interfacial Electrochem.*, 1992, **338**, 86.